Journal of African Earth Sciences 79 (2013) 10–23

Contents lists available at SciVerse ScienceDirect

Journal of African Earth Sciences

journal homepage: www.elsevier.com/locate/jafrearsci

Remobilisation features and structural control on ore grade distribution at the Konkola stratiform Cu–Co ore deposit, Zambia

K. Torremans [a,*], J. Gauquie [a], A.J. Boyce [b], C.D. Barrie [b,c], S. Dewaele [d], O. Sikazwe [e], Ph. Muchez [a]

[a] Geodynamics and Geofluids Research Group, Department of Earth and Environmental Sciences, KU Leuven, Celestijnenlaan 200E, B-3001 Leuven, Belgium
[b] Scottish Universities Environmental Research Centre, Rankin Avenue, Scottish Enterprise Technology Park, East Kilbridge G75 0QF, Scotland, UK
[c] Isoprime Ltd., Isoprime House, Earl Road, Cheadle Hulme, Cheadle SK8 6PT, UK
[d] Department of Geology and Mineralogy, Royal Museum of Central Africa (RMCA), Leuvensesteenweg 13, 3080 Tervuren, Belgium
[e] University of Zambia, School of Mines, Geology Department, P.O. Box 32379, Lusaka, Zambia

ARTICLE INFO

Article history:
Received 4 April 2012
Received in revised form 4 October 2012
Accepted 13 October 2012
Available online 2 November 2012

Keywords:
Stratiform Cu–Co ore deposits
Structural control
Remobilisation
Konkola
Central African Copperbelt

ABSTRACT

The Konkola deposit is a high grade stratiform Cu–Co ore deposit in the Central African Copperbelt in Zambia. Economic mineralisation is confined to the Ore Shale formation, part of the Neoproterozoic metasedimentary rocks of the Katanga Supergroup. Petrographic study reveals that the copper–cobalt ore minerals are disseminated within the host rock, sometimes concentrated along bedding planes, often associated with dolomitic bands or clustered in cemented lenses and in layer-parallel and irregular veins. The hypogene sulphide mineralogy consists predominantly of chalcopyrite, bornite and chalcocite. Based upon relationships with metamorphic biotite, vein sulphides and most of the sulphides in cemented lenses were precipitated during or after biotite zone greenschist facies metamorphism. New $\delta^{34}S$ values of sulphides from the Konkola deposit are presented. The sulphur isotope values range from −8.7‰ to +1.4‰ V-CDT for chalcopyrite from all mineralising phases and from −4.4‰ to +2.0‰ V-CDT for secondary chalcocite. Similarities in $\delta^{34}S$ for sulphides from different vein generations, earlier sulphides and secondary chalcocite can be explained by (re)mobilisation of S from earlier formed sulphide phases, an interpretation strongly supported by the petrographic evidence. Deep supergene enrichment and leaching occurs up to a km in depth, predominantly in the form of secondary chalcocite, goethite and malachite and is often associated with zones of high permeability. Detailed distribution maps of total copper and total cobalt contents of the Ore Shale formation show a close relationship between structural features and higher copper and lower cobalt contents, relative to other areas of the mine. Structural features include the Kirilabombwe anticline and fault zones along the axial plane and two fault zones in the southern limb of the anticline. Cobalt and copper behave differently in relation to these structural features. These structures are interpreted to have played a significant role in (re)mobilisation and concentration of the metals, in agreement with observations made elsewhere in the Zambian Copperbelt.

1. Introduction

The Central African Copperbelt is one of the largest and richest metallogenetic provinces in the world (Cailteux et al., 2005; Hitzman et al., 2005; Selley et al., 2005). Geographically it straddles the border between Zambia and the Democratic Republic of Congo (Fig. 1). Throughout the years, different metallogenetic models have been proposed for the ore deposits in the Central African Copperbelt (for reviews see Cailteux et al., 2005; El Desouky et al., 2010; Selley et al., 2005). Several recent studies agree that most of the high grade Cu–Co deposits formed via a multiphase system with several early to late diagenetic and synorogenic mineralisation and mobilisation stages (Cailteux et al., 2005; Haest and Muchez, 2011; Muchez et al., 2010; Selley et al., 2005). However, to date this model is not yet generally accepted (Sillitoe et al., 2010).

The Konkola deposit has been the subject of intensive research in the past. Several authors have investigated the local geology, petrology and the type and occurrence of mineralisation as well as indications for the sedimentological and palaeo-environment at Konkola (e.g. Fleischer et al., 1976; Katongo, 2005; Mulenga et al., 1992; Ralston, 1963; Raybould, 1978; Schwellnus, 1961). A study of boreholes from the Konkola deposit was carried out to evaluate the role of diagenetic processes in ore formation by analysis of mineralogical, geochemical and stable isotope data (Sweeney and Binda, 1989; Sweeney et al., 1986). The Konkola

* Corresponding author. Address: Celestijnenlaan 200E, 02.217 3001 Leuven, Belgium. Tel.: +32 16 3 26448/473 66 71 73.
E-mail addresses: koen.torremans@ees.kuleuven.be (K. Torremans), adrian.boyce@glasgow.ac.uk (A.J. Boyce), craig.barrie@isoprime.co.uk (C.D. Barrie), stijn.dewaele@africamuseum.be (S. Dewaele), osikazwe@unza.zm (O. Sikazwe), philippe.muchez@ees.kuleuven.be (Ph. Muchez).

1464-343X/$ - see front matter © 2012 Elsevier Ltd. All rights reserved.
http://dx.doi.org/10.1016/j.jafrearsci.2012.10.005

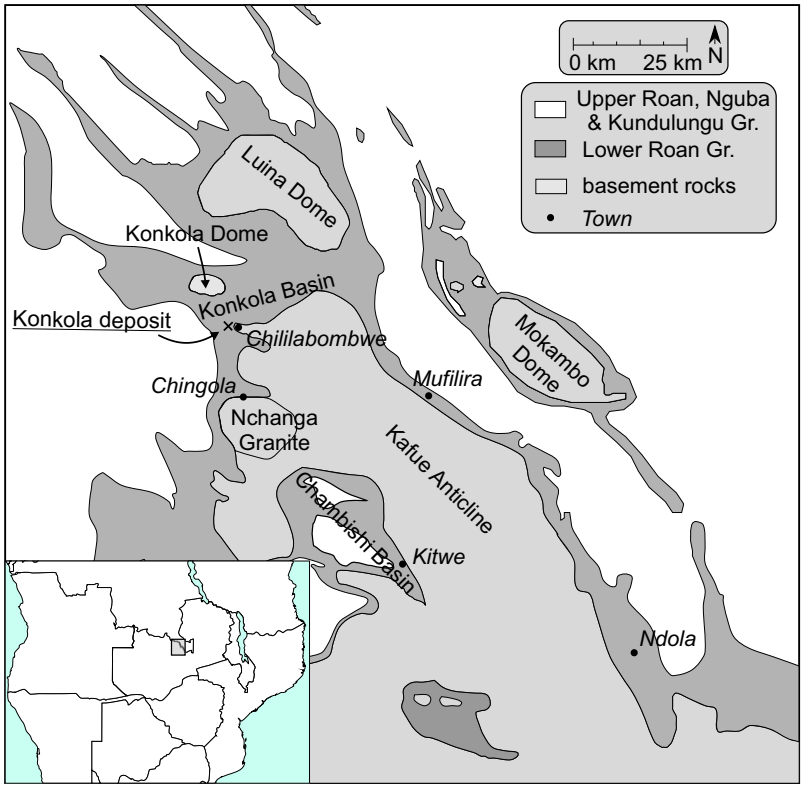

Fig. 1. Geological map of the eastern part of the Zambian Copperbelt. Modified from Ralston (1963), Cailteux et al. (2005) and Selley et al. (2005). Inset shows the geographical position in southern Africa. Gr. = Group.

deposit has also been the subject of more holistic studies of the Copperbelt (e.g. Cailteux et al., 2005; Selley et al., 2005).

Ore deposit research often attempts to quantify ore distribution and its relationship to lithology, structural features, alteration, metamorphism and deformation. These relationships are of great importance and essential for the mining and exploration industry. Earlier research at Konkola has indicated a predominantly early diagenetic origin for the Cu–Co ore (Sweeney and Binda, 1989; Sweeney et al., 1986) although several authors have indicated that other processes played a role in upgrading the ore at Konkola to present values (Fleischer et al., 1976; Ralston, 1963; Raybould, 1978). It is, however, unclear to what extent these processes are important because no systematic study of the relationship between ore grade distribution and the different geological characteristics has been carried out.

The aim of this study is to investigate the factors controlling ore distribution and mineralisation at Konkola mine. Insights are gained in the formation conditions and subsequent (re)crystallisation and (re)mobilisation processes that affected the deposit, based on petrographical, structural and geochemical/isotopic observations. Fieldwork at Konkola involved logging of drill cores, description and sampling of underground crosscuts and study of detailed 1:250 scale mine maps and borehole logs.

2. Geological context and geodynamic history

The stratiform Cu–Co deposits of the Central African Copperbelt are hosted in the Neoproterozoic metasedimentary rocks of the Katanga Supergroup (Selley et al., 2005), which is subdivided into the Roan, Nguba and Kundulungu Groups, based upon the presence of glacial diamictites (Bull et al., 2011; Cailteux et al., 1994). The youngest igneous activity before deposition of the Katanga Supergroup is the intrusion of the Nchanga granite into the pre-existing basement at 883 ± 10 Ma (Armstrong et al., 2005; Master et al., 2005), which provides an important maximum age for the start of deposition of the Katanga Supergroup. Sedimentation of the Mindola Clastics Subgroup commenced after this intrusion, with arkosic sandstones and immature conglomerates. These were deposited in fault-related sub-basins (Selley et al., 2005) in response to continental rifting associated with the breakup of Rodinia (Meert and Torsvik, 2003; Tembo et al., 1999).

The Mindola Clastics Subgroup is conformably overlain by the Kitwe Subgroup, which is locally subdivided into the Ore Shale, Pelitico-Arkosic and Chingola formations (Table 1). These formations mainly consist of carbonates and siliciclastic rocks (Cailteux et al., 1994; Porada and Berhorst, 2000) and contain the Cu–Co mineralisation (Selley et al., 2005). The Ore Shale formation, which hosts the main Cu–Co mineralisation at the Konkola deposit, occurs at the transition from basal continental clastics to shallow marine rocks and marks a fundamental change in basin configuration (Bull et al., 2011; Selley et al., 2005). The overlying formations of the Roan Group consist of a variety of lithologies, with sandstones, dolomites and shales in a "layer-cake morphology" (Selley et al., 2005). A period of relative tectonic quiescence coincided with formation of the carbonate platforms of the Kirilabombwe Subgroup (Bull et al., 2011; Porada and Berhorst, 2000). The Mwashya rocks are either placed as a Subgroup at the top of the Roan Group (Batumike et al., 2006; Bull et al., 2011; Cailteux et al., 1994, 2007; Kampunzu and Cailteux, 1999), as a separate Group (Porada and Berhorst, 2000; Selley et al., 2005; Sutton and Maynard, 2005) or as the lowermost Subgroup of the Nguba Group (Master et al., 2005; Master and Wendorff, 2011; Wendorff, 2005; Wendorff and Key, 2009). However, a discussion on the stratigraphy is beyond the scope of this paper. Continued basin development during deposition of carbonates and siliciclastics of the Nguba Group (Batumike et al., 2007) subsequently resulted in a

Table 1
Lithostratigraphy of the Roan Group at Konkola, with reference to the general stratigraphy of the Zambian Copperbelt (after Bull et al., 2011; Cailteux et al., 1994, 2007; Konkola Copper Mines, 2010; Selley et al., 2005; Sweeney et al., 1986). Pelito-Arkosic and Ore Shale formations do not conform to the IUGS code of lithostratigraphic nomenclature. However they are frequently used in the literature and are hence bracketed.

Group	Sub group	Formation	Local terminology	Thickness (m)	Lithology
Roan ~1050–2300 m	Mwashia		Mwashia Shale	300–600	Black to dark grey carbonaceous shales, dolomitic shales, arenites and arkoses
	Kirila bombwe	Kanwangungu	Upper Roan Dolomite	100–450	Dolomites and dolomitic siltstones
		Kibalongo	Shale with Grit	40–165	Gritty shales (*cfr*. Antelope Clastics)
	Kitwe	Chingola	Hanging Wall Aquifer	20–60	Dolomites and sandstones with argillite beds on top
		(Pelito-Arkosic)	Hanging Wall Quartzite	10–150	Coarse-grained feldspathic arenites and arkoses with argillites and dolomitic argillites
		(Ore Shale)	*Ore Shale*	4–20	
			Units		
			E		Micaceous siltstone and brown feldspathic sandstones that become pronounced towards top.
			D		Gradational transition from basal siltstone with lenses of carbonaceous sandstone to thinly bedded coarser siltstone with lenses of carbonaceous feldspathic sandstone.
			C		
			B		Massive finegrained siltstone
			A		Laminated siltstone and dolomite
	Mindola Clastics	Mutonda	Footwall Conglomerate	20–40	Conglomerates, coarse arkoses
			Footwall Sandstone		Arkosic sandstones
			Porous Conglomerate		Pebble and cobble conglomerates
			Argillaceous Sandstone	400	Argillites and sandstones
		Kafufya	Footwall Quartzite		Arkoses and sandstones
		Chimfunsi	Lower Porous Conglomerate	30	Pebble and cobble conglomerate
			Pebble Conglomerate	30–40	
			Boulder Conglomerate	100–300	

progressive evolution to a mature proto-oceanic rift (Kampunzu et al., 2000; Key et al., 2001; Porada and Berhorst, 2000). Fault arrays that were present during the continental rift stage integrated into larger master faults (Cailteux et al., 2005; Selley et al., 2005). $^{40}Ar/^{39}Ar$ dating of detrital muscovite grains from the Biano Subgroup at the top of the Kundulungu Group (Cailteux et al., 2007) at 573 ± 5 Ma provides a minimum age for the Katanga Supergroup (Master et al., 2005).

Formation of Gondwana and collision of the Congo-Tanzania and Angola-Kalahari cratons caused inversion of the Katangan basin (De Waele et al., 2008; John et al., 2004). The timing of the resulting Lufilian orogeny is estimated at ca. 595–490 Ma (Selley et al., 2005) with maximum metamorphism taking place at ~530 Ma (John et al., 2004; Rainaud et al., 2005). Associated northwest to northeast directed thrusting caused tectonic displacement perpendicular to the arcuate shape of the Lufilian orogenic belt (Cosi et al., 1992; Kampunzu and Cailteux, 1999; Porada and Berhorst, 2000; Selley et al., 2005).

3. The Konkola ore deposit

The Konkola copper–cobalt deposit is a high-grade stratiform deposit in the eastern part of the Zambian Copperbelt (Fig. 1). The deposit contains 228 Mt of reserves and resources at an average grade of 3.6 wt% Cu (Vedanta, 2010). There is some confusion in the literature concerning the nomenclature of deposits in the greater Konkola region. The Musoshi ore deposit is situated on the north side of the Konkola Dome (Fig. 2; cf. Richards et al., 1988) and the Konkola North deposit on the southeastern side of this dome (cf. Sutton and Maynard, 2005). In this paper we discuss the Konkola deposit, lying adjacent to the Chililabombwe Dome (cf. Selley et al., 2005; Sweeney and Binda, 1989; Sweeney et al., 1986). In the older literature the deposit is called the Bancroft deposit (e.g. Dechow and Jensen, 1965; Ralston, 1963; Schwellnus, 1961) and is described as consisting of two orebodies separated by a barren gap (e.g. Fleischer et al., 1976). This barren gap is, however, continuous below a depth of 720 m from the surface (Katongo, 2005), rendering a strike length of >10 km of resources at a cut off grade of 1 wt% Cu.

In the Copperbelt, different stratigraphical unit names have been applied to the same rock masses in literature. Some authors assign 'formation' as term for a given rock unit (Bull et al., 2011; Selley et al., 2005) whereas others use 'subgroup' as unit term for the same rock unit (Cailteux et al., 2005, 2007; Porada and Berhorst, 2000). A detailed description of the lithologies at Konkola and a correlation between locally defined units and formal units is given in Table 1. Economic copper mineralisation at Konkola is generally restricted to the Ore Shale formation and to adjacent parts of formations above and below the Ore Shale. The Ore Shale formation rests conformably on the Mindola Clastics Subgroup and has a variable thickness of 4–20 m. Formations of the Mindola Clastics Subgroup show important thickness and lateral facies changes, typical for sediments deposited in fault-bounded rift basins of the Mindola Clastics Subgroup (Bull et al., 2011; Selley et al., 2005). The Ore Shale formation is a finely laminated, dark grey siltstone to fine sandstone with important dolomitic bands and some lateral facies variations (Konkola Copper Mines, 2010). At Konkola, the Ore Shale formation is subdivided into five units, A to E. Mineralisation occurs disseminated in the matrix of the host rock mainly as chalcopyrite, bornite and chalcocite (Sweeney et al., 1986). Important concentrations of sulphides also occur in dolomitic bands, cemented lenses and layers and in layer-parallel and irregular, sometimes massive veins (Konkola Copper Mines, 2010; Ralston, 1963; Schwellnus, 1961). The ore deposit was subjected to different alteration and supergene processes (Fleischer et al., 1976; Ralston, 1963).

4. Structural setting

The Konkola ore deposit is draped around the Kirilabombwe anticline (Figs. 3 and 7). In the core of the anticline are the Proterozoic basement rocks of the Kirilabombwe Dome, contiguous to the basement complex of the Kafue Anticline (Fig. 2; Ralston, 1963; Raybould, 1978; Sweeney et al., 1986). The Katanga Supergroup strata are deformed together with the basement rocks (Selley

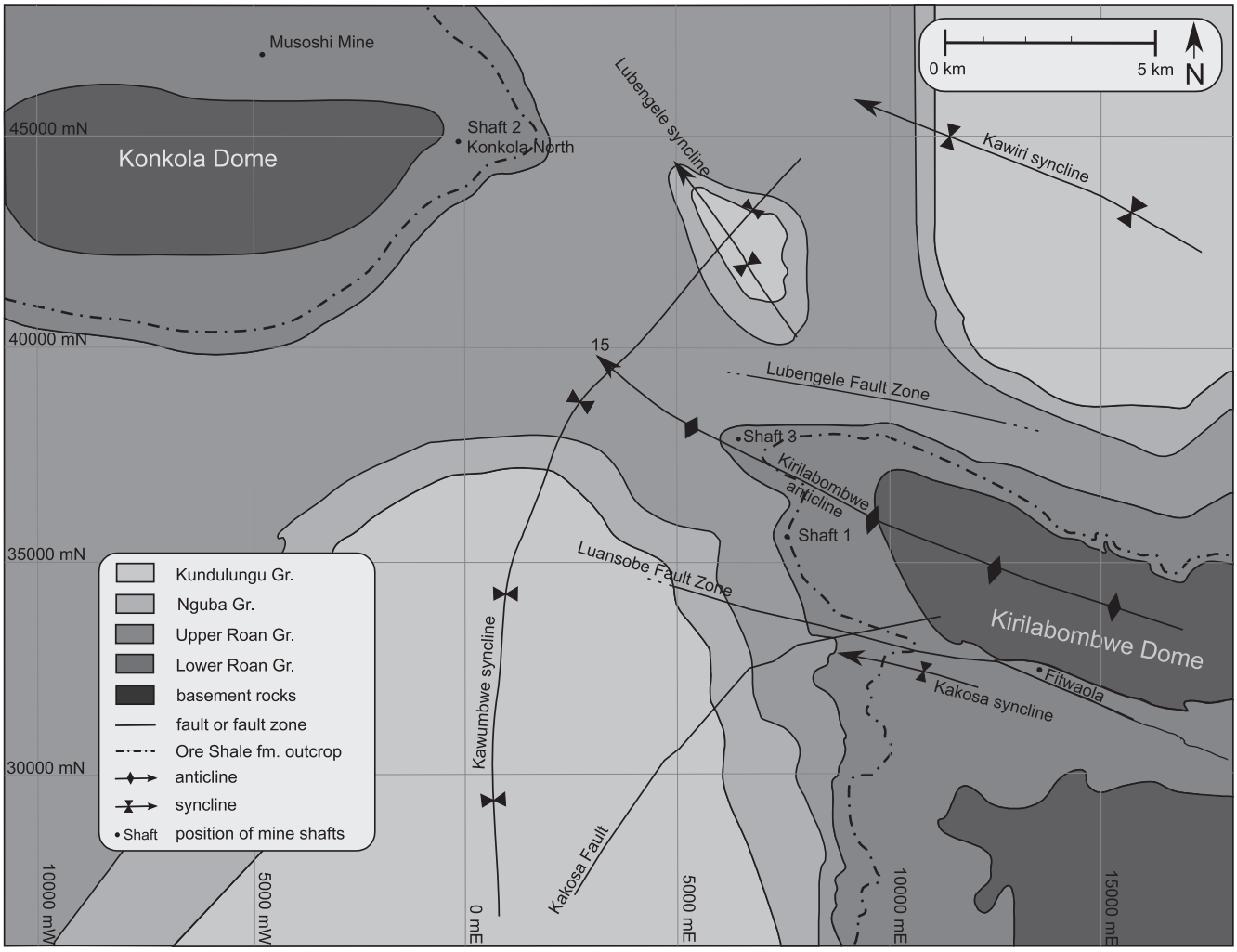

Fig. 2. Geological map of the greater Konkola area. The Konkola ore deposit is adjacent to the Kirilabombwe Dome. The Musoshi and Konkola North ore deposits are situated next to the Konkola Dome. Modified from Konkola Copper Mines (2010). Gr. = Group.

et al., 2005). The Kawumbwe syncline and Kirilabombwe anticline form a structural saddle between the Kirilabombwe and Konkola basement domes (Fig. 2). Analysis of boreholes along the axis of the anticline and in situ measurements show that the Kirilabombwe anticline plunges at 10–15° to the northwest with a N75W strike of the fold axis (Fig. 3B). It is a tight and upright anticline with a subvertical axial plane and an interlimb angle of 35–45°.

Important fault zones, up to 60 m wide, occur on the southern limb of the anticline at 2200 mN and 2700 mN (Fig. 3). These NE–SW trending fault zones are bounded by two major fault planes dipping on average ~75–85° to the north, with parallel secondary faults in between. The faults extend from the surface to well into the footwall formations at 1 km depth (Katongo, 2005). A fault zone, termed the Kirilabombwe fault, runs parallel to the axial plane of the anticline (Ralston, 1963). A zone of secondary folding in the south of the deposit – 500 mN to 500 mS at present day mining levels (~600–1000 m depth) – consists of multiple upright low amplitude gently north to northwest plunging folds (10–30°). These folds were also described at higher mining levels which are no longer accessible (from near surface down to ~600 m depth; Fleischer et al., 1976; Ralston, 1963; Schwellnus, 1961). Two important fault zones also occur to the north and south ends of the deposit (Fig. 3). The Lubengele fault zone consists of faults dipping 79° to the south and the Luansobe fault zone of faults dipping 82° to the north (Mulenga et al., 1992).

5. Petrography

5.1. Methodology

Boreholes KLB146A (7423.54 mE, 33062.73 mN starting from 1283.11 m above sea level with a total length of 734.26 m) and KLB147 (7552.46 mE, 33611.15 mN starting from 1286.76 m above sea level with a total length of 1031.00 m) were studied and sampled for an overview of the complete stratigraphy. Three assay boreholes BPN854 (4700 mN on 2340 L, in feet), BV1464 (196 mN on 960 mL, in metre) and BV1465 (198 mN on 985 mL, in metre) were described in detail macroscopically to investigate the Ore Shale and surrounding metres of the hangingwall and footwall formations. In addition, several crosscuts, covering representative parts of the mine, were logged, mapped and sampled in detail. All samples of the mineralised areas that were studied at KU Leuven were taken underground on fresh surfaces of recently developed mining crosscuts going through the entire Ore Shale formation and parts of the footwall and hanging wall formations. The location of these crosscuts in local mine coordinates are 4100 mN, 4300 mN, 4700 mN at 2340 L (feet), 4300 mN at 2410 L (feet), 2656 mN at 2650 L (feet), 190 mS at 1000 mL (metre), 850 mS at 2950 L (feet) and 1200 mS at 3150 L (feet).

A petrographic study was carried out on 53 thin sections and 18 polished sections using an Olympus BX60 microscope. Photomicro-

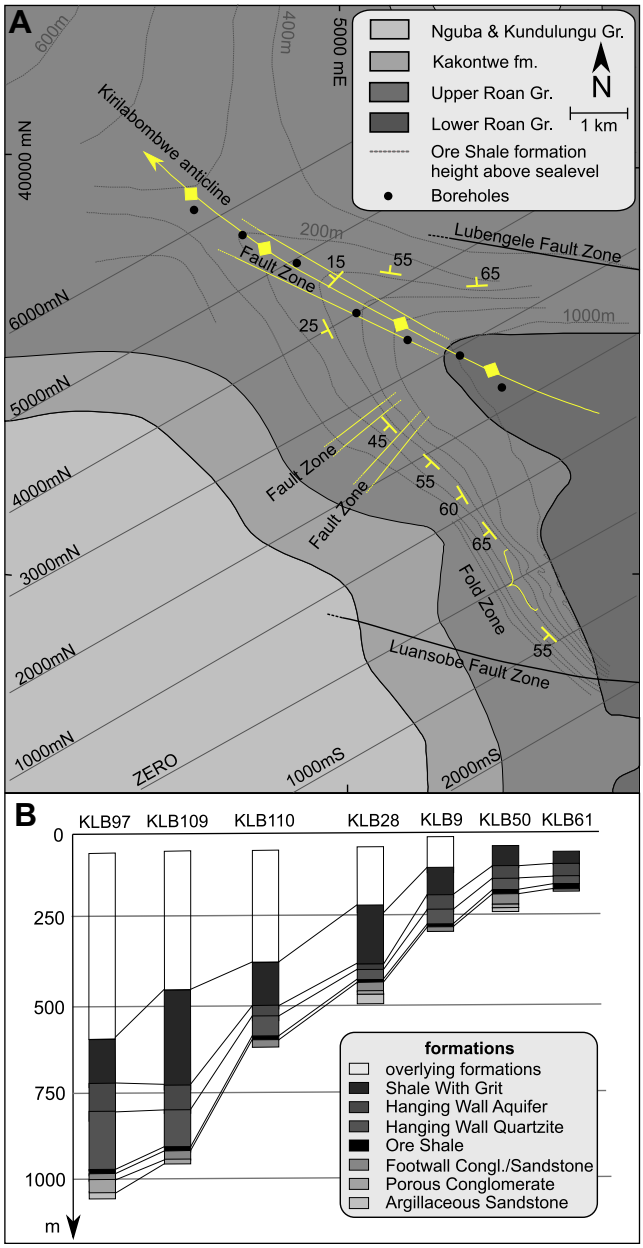

Fig. 3. Map of structural elements associated with the Konkola ore deposit (A) and selected boreholes along the axis of the Kirilabombwe anticline (B). Position of the boreholes is indicated in (A). Modified from Konkola Copper Mines (2010). Legend is similar to Fig. 2. Gr. = Group; Fm. = Formation.

graphs were taken with a Deltapix DP200 image capturing system. Cold cathode luminescence of samples was studied using a Technosyn Cold Cathode Luminescence Model 8200 Mk II combined with a Nikon microscope and a ProgRes C10 image capturing system. Working conditions were between 7 to 11 kV and 400 to 700 μA with a beam width of 5 mm at a vacuum of 5.5 Pa. To identify the type of carbonates, samples were stained and rocks that were too fine for petrographic analysis were studied via X-ray powder diffraction.

5.2. Results

5.2.1. Host rock, cemented layers and metamorphic minerals

A general paragenesis for the Konkola deposit has been constructed based on our study of boreholes, underground crosscuts and detailed petrography on thin and polished sections (Fig. 4). Constituents of the host rock (matrix) are not shown in the paragenesis but described in the text. The matrix of the host rock consists of a detrital framework of subrounded to rounded dull purple luminescent quartz, bright blue luminescent feldspar, phyllosilicates and accessory zircon, tourmaline, apatite and Ti-oxides. The feldspar grains were identified as anorthoclase and microcline. Detrital elongated muscovite grains are strongly aligned along bedding planes and sometimes bent around the edges of other crystals.

Important amounts of authigenic non-luminescent quartz, microcline and albite occur as overgrowths on detrital grains or as a cement in the host rock. Detrital quartz and feldspar grains are corroded by the authigenic overgrowths. This cementation appears to be particularly concentrated in certain parts of the host rock, forming lenses and layers that range in size from millimetre sized spots to structures with irregular boundaries that extend laterally over several tens of centimetres. These are further termed cemented lenses (Fig. 5D). The authigenic overgrowths show important but complicated timing relationships with authigenic microcline often overgrowing and engulfing authigenic quartz and dolomite. Dolomitisation is identified to occur both prior to and after authigenic quartz and feldspar overgrowths.

Dolomitic bands regularly occur in the Ore Shale units C and D. The transition between these bands and the surrounding host rock can be both gradual and abrupt. Dolomitic bands contain abundant dolomite that occurs as a pervasive matrix cement as well as quartz with undulose extinction and plagioclase and microcline. Different phases of dolomitisation have affected the Ore Shale. Most of the dolomite is identified to be Fe-rich and is either (1) dull brown or (2) bright orange luminescent. A later phase of strongly zoned yellow to bright orange luminescent carbonate fills pores and cracks and can in places completely replace the matrix. This type of carbonate appears to be restricted to permeable zones, including fault zones.

Biotite and muscovite are important constituents of the Ore Shale. These phyllosillicates are disseminated in the host rock or occur in clusters or lined up along bedding planes (Fig. 5B). Long (100–400 μm) muscovite laths are often overgrown and replaced by biotite (Fig. 5B). The muscovite laths are almost invariably larger than their biotite overgrowths (Fig. 5B). These phyllosilicate overgrowths are interpreted to have formed during metamorphism and show important crosscutting relationships with sulphides and other minerals.

5.2.2. Ore mineralogy and its relationship to other minerals

The copper–cobalt ore minerals occur (1) disseminated in the host rock (Fig. 5A), (2) as clusters in cemented lenses (Fig. 5C and D) and (3) in layer-parallel or irregular veins (Fig. 5E and F). The sulphides in the host rock are randomly disseminated or concentrated along bedding planes or in dolomitic bands (Fig. 5A). The mineralogy of these sulphides is dominated by chalcopyrite, bornite and chalcocite with relative abundance varying greatly. Where the term chalcocite is used, it refers to the chalcocite-group minerals (Ramdohr, 1980; Sillitoe, 2005). The ore minerals are irregular in shape and are often intergrown with each other. Some minor carrollite and accessory sub- to euhedral pyrite are present. The grain size of the disseminated sulphides appears to be related to the grain size of the host rock.

Important amounts of sulphides are found in the cemented lenses and layers where they are interstitial to and corrode authigenic quartz, microcline and dolomite (Fig. 5C). These cross-cutting relationships are most obvious in the most coarse-grained cemented layers where the size of the sulphides can be >500 μm, sometimes filling large parts of the structures (Fig. 5C). In some of the smaller or irregular lenses, authigenic quartz and feldspar are seen to completely engulf some of the finer grained chalcopyrite (Fig. 5D). Therefore sulphides occur both before and after

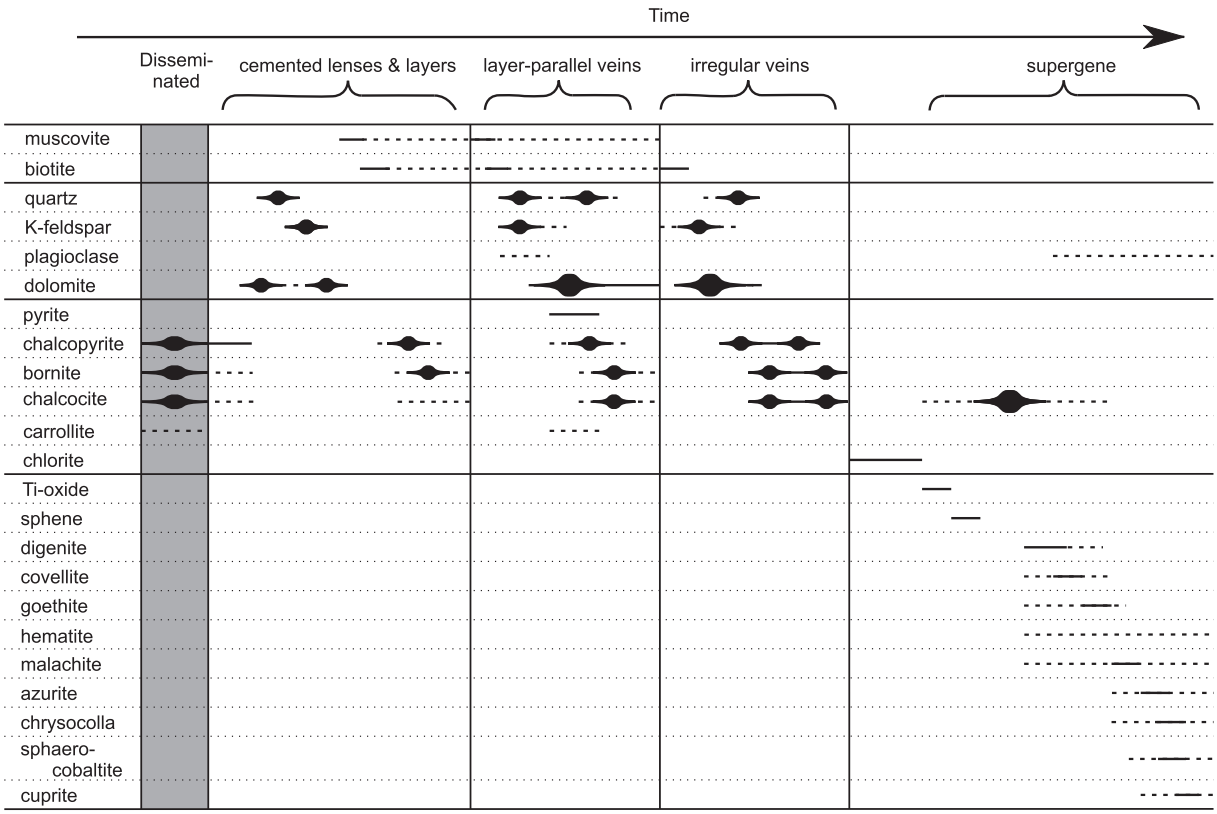

Fig. 4. General paragenesis for the Ore Shale formation, based on our study of boreholes, underground crosscuts and detailed petrography on thin and polished sections. Constituents of the host rock (matrix) are not shown but described in the text.

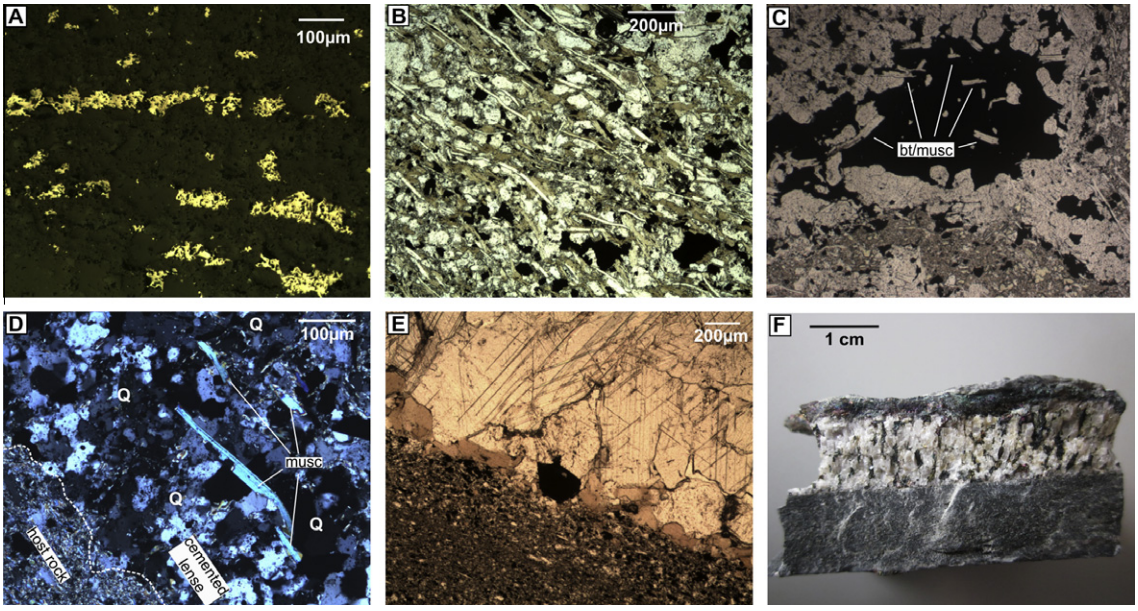

Fig. 5. Microphotographs of thin sections, with exception of (F). PPL = plane polarised light; XPL = crossed polarised light; IL = incident light. (A) Disseminated chalcopyrite in host rock, slightly concentrated along bedding planes, IL. (B) Muscovite with biotite overgrowths crosscutting previous phases in the Ore Shale formation, such as authigenic quartz and feldspar, PPL. (C) Cemented lense in the Ore Shale formation. Muscovite with biotite overgrowths is enclosed in chalcopyrite, PPL. (D) Contact between cemented lense and host rock. Muscovite overgrows chalcopyrite and authigenic quartz, XPL. (E) Contact between siltstone host rock and layer-parallel vein. Biotite is concentrated on the rim of the vein. Quartz and feldspar are subhedral phases on the vein wall and twinned dolomite is the younger phase towards the middle of the vein, PPL. (F) Hand specimen of layer-parallel vein with elongated dolomite crystals and bornite that is interstitial to the dolomite.

precipitation of authigenic quartz, feldspar and dolomite. Chalcopyrite, chalcocite and bornite are the main ore minerals in the cemented lenses and are often intergrown. Bornite can be altered to chalcopyrite at mineral edges and while the opposite is also apparent, it is much rarer. Later digenite, covellite, chalcocite and goethite replace chalcopyrite and bornite along crystal edges

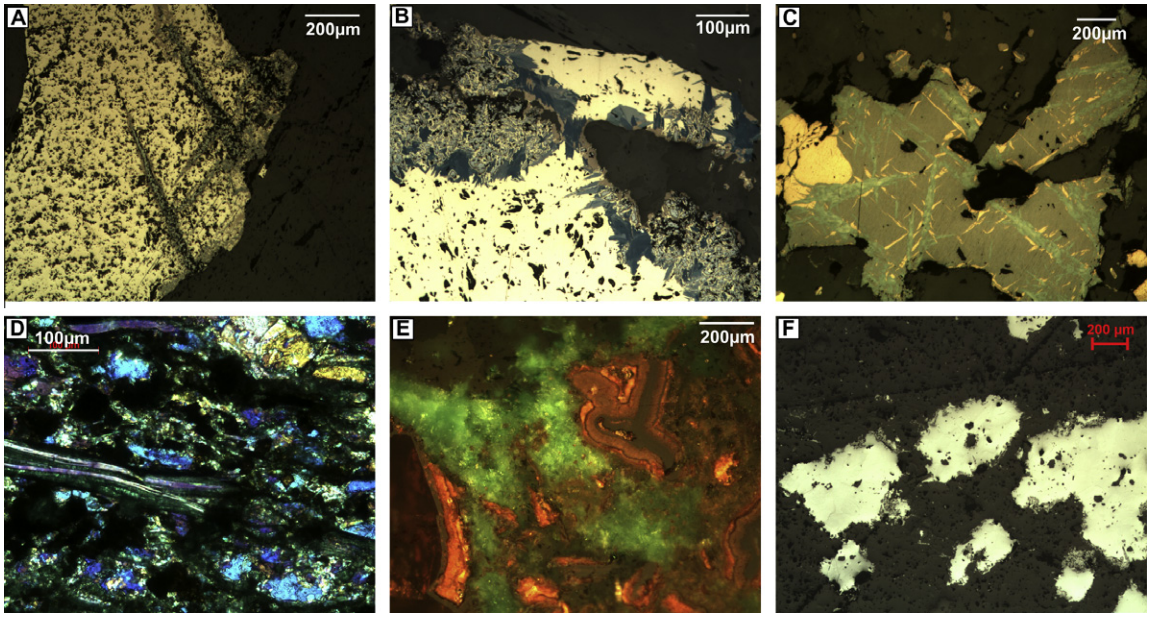

Fig. 6. Microphotographs of polished sections and a thin section (D). XPL = crossed polarised light; IL = incident light; IPL = double polarised incident light; PPL = plane polarised light. (A) Goethite in crack after digenite in chalcopyrite matrix. Bornite is later alteration, IL. (B) Irregular vein with coarse chalcopyrite with bornite, covellite, chalcocite and goethite alteration on the edges, IL. (C) Chalcopyrite, bornite and digenite in layer-parallel vein with digenite and chalcopyrite exsolution lamellae in bornite, IL. (D) Biotite that is replaced by malachite along cleavage, XPL. (E) Banded goethite with malachite in pores, IPL. (I) Secondary chalcocite filling pores and associated with goethite rims, IL.

(Fig. 6B) or along cracks in the minerals (Fig 6A). Rare euhedral pyrite cubes are almost invariably surrounded by bornite rims in a chalcopyrite matrix.

Some phyllosilicates overgrow small sulphides as well as authigenic silicates that in their turn engulf and post-date these small sulphides (Fig. 5D). This implies that these sulphides formed prior to metamorphism. However, in the majority of cemented lenses and also in veins, sulphides overgrow muscovite and biotite (Fig. 5C). The phyllosilicates occur engulfed by the sulphides (Fig 5C), intergrown with them, and intruded and corroded by the sulphide phases. Furthermore the phyllosilicates are often abruptly cross-cut by the sulphide phases. As these lenses and veins often contain important amounts of sulphides, this implies that the majority of sulphides formed during or after metamorphism. Fan-shaped chlorite is sometimes found, replacing biotite or growing in pores.

5.2.3. Veins in the Ore Shale formation

The Ore Shale formation at Konkola contains layer-parallel veins. These veins continue for several metres along bedding planes with thicknesses mostly <2 cm (Fig. 5F). The veins often, but not exclusively, form at the contact between coarse-grained and fine-grained layers. The main gangue minerals are dolomite, quartz and microcline with dolomite as the predominant mineral (Fig. 5E). Crystal growth is from the edges inwards with sub- to euhedral dull luminescent quartz and smaller (generally <100 µm) blocky crystals of microcline and plagioclase (Fig. 5E). Minor biotite (150–250 µm) and accessory muscovite and chlorite are present. Unoriented masses of biotite and muscovite often occur on the edges of the veins (Fig. 5E). Very coarse subhedral dull brown luminescent dolomite ($\geqslant$200 µm up to over a millimetre) corrodes, engulfs and thus postdates all phases on vein walls (Fig. 5E). This dolomite is Fe-rich and generally strongly twinned and fractured, with individual twin widths up to several microns (Fig. 5E). Small (50–200 µm) subhedral quartz crystals occur as inclusions in or between individual dolomite crystals.

The sulphide minerals in the veins are chalcopyrite, bornite and chalcocite with minor subhedral pyrite. The sulphides can be interstitial to dolomite or can intrude and cross-cut dolomite along crystal cleavage planes. The sulphides occur late in the paragenesis of the veins and typically, but not always, postdate the coarse dolomite and previous phases. Sulphides can also be massive, almost filling up entire veins. It is often unclear what the exact temporal relationship between chalcopyrite, bornite and chalcocite is. In some cases, bornite replaces chalcopyrite but in others, the opposite is apparent. Generally, however, the bulk of chalcopyrite is identified as forming first with bornite later replacing this phase. Occasionally, euhedral pyrite cubes with bornite overgrowths occur within chalcopyrite. Ore textures are complex and include exsolution lamellae of chalcopyrite in bornite (Fig. 6C), bornite in chalcopyrite, digenite in bornite (Fig 6C) and chalcocite in digenite. Replacive textures include minor digenite, covellite, goethite and chalcocite that alter bornite from the edges (Fig 6B). Cracks within chalcopyrite grains are frequently filled by successive goethite, bornite and digenite (Fig. 6A).

Some layer-parallel veins contain dolomite crystals that are elongated perpendicular to bedding with an aspect ratio <0.2 (Fig 5F). In these veins, successive generations of vein growth can be seen, with ore phases precipitated in between successive phases. Fragments of the host rock are occasionally enclosed parallel to the vein walls. In rare cases, the veins are completely filled with coarse-grained blocky crystals of microcline and dolomite.

The layer-parallel veins are crosscut by several generations of irregular veins, showing no systematic orientation. Their thickness varies greatly from hairline sub-millimetre sized veins up to 10 cm thick veins. Gangue minerals are similar to those in the layer-parallel veins with euhedral quartz, dolomite and microcline crystals up to several centimetres in size. Microcline crystallised before quartz and dolomite. Ore mineralogy in the irregular veins is similar to the cemented lenses and layer-parallel veins. When irregular veins crosscut mineralised bedding, ore minerals are present in large quantities in the veins. In other cases, they contain only minor mineralisation or lack any visible mineralisation. In both the

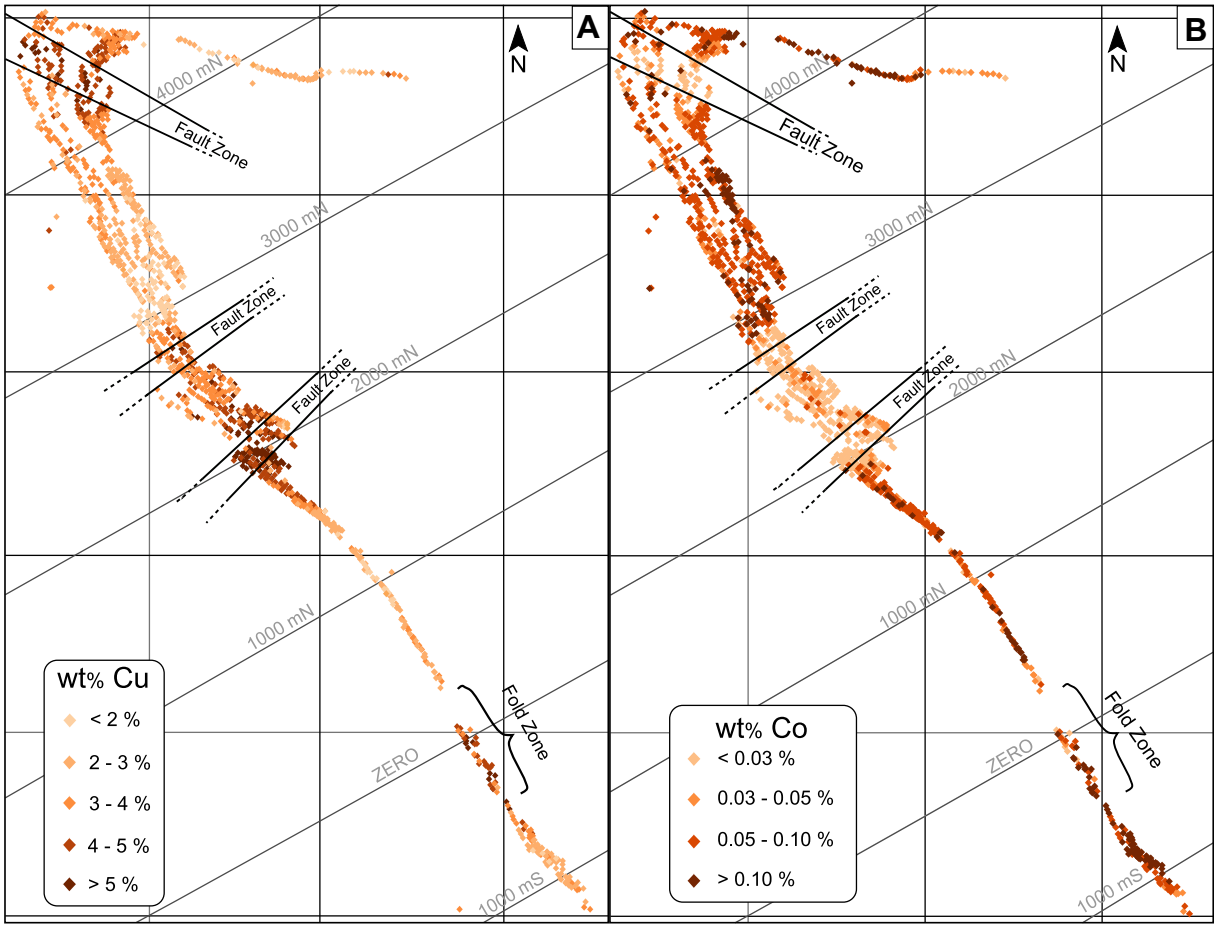

Fig. 7. Grade maps of the Konkola ore deposit of the total copper (A) and total cobalt (B) contents in weight percent (wt%), averaged over the thickness of the Ore Shale formation. Several exploitation levels are projected on the maps. All assay analyses were done by Konkola Copper Mines (2010).

layer-parallel and irregular veins, dolomite can be strongly twinned and often shows fractures. Biotite and muscovite are sometimes observed, lined up along the rims of the veins.

5.2.4. Evidence for supergene processes

Important secondary porosity is recognised in the Ore Shale and is most pronounced in dolomitic bands near permeable zones. Goethite, secondary chalcocite and malachite often fill this secondary porosity in an irregular and patchy manner (Fig. 6E). Supergene mineralisation extends up to a km in depth from the surface and occurs in the form of malachite, digenite, covellite, azurite, chrysocolla, sphaerocobaltite ($CoCO_3$), goethite and secondary chalcocite. Malachite and chalcocite are the most common supergene copper minerals at Konkola with the former occurring as: (1) thin stringers following but also cross-cutting bedding planes, (2) intruding biotite or muscovite along cleavage (Fig. 6D), (3) pervasive in the matrix and (4) aggregated, often associated with goethite and chalcocite in pores and cavities (Fig 6E). Goethite directly replaces primary sulphides or is precipitated as patches filling secondary porosity and cracks (Fig. 6E).

Secondary chalcocite (Fig. 6F) can be tentatively distinguished from primary chalcocite on a textural basis, its association with goethite or hematite, the filling of secondary porosity, an often aggregate crystal habit or the absence of intergrowths with hypogene bornite or chalcopyrite (cf. Clark et al., 2001; Sillitoe, 2005). Based on these criteria, a distinction was made between hypogene and supergene chalcocite. Hexagonal chalcocite and the presence of inversion lamellae in chalcocite are evidence of formation at temperatures higher than 103 °C. Orthorhombic chalcocite can form as a supergene mineral but also as hypogene crystals at temperatures lower than 103 °C (Fleet, 2006; Ramdohr, 1980). Orthorombic chalcocite lacks the growth lamellae of hexagonal chalcocite. No growth lamellae were observed in any of the studied chalcocites. Secondary chalcocite occurs disseminated in the Ore Shale as patches filling up secondary porosity or as massive aggregate infills (Fig. 6F). Secondary chalcocite is also often associated with permeable layers and areas, such as fault zones and is particularly abundant in dolomitic bands near those areas.

6. Ore distribution

6.1. Methodology

To assess ore distribution at Konkola, grade maps were produced for total copper, total cobalt and acid soluble copper content, all expressed in weight percent (wt%) averaged over the complete thickness of the Ore Shale formation. These maps contain 1458 data points, producing a 2D planar view of the ore grade distribution, projected from the different mine levels (Fig. 7). The method used to obtain total copper, cobalt and acid soluble copper was atomic absorption spectrometry (AAS). All chemical analyses were carried out at the chemical laboratory of Konkola Copper Mines. These measurements were assay results used in mine and production planning.

6.2. Results

The grade maps show considerable variation in copper grades along strike of the deposit (0–5 wt%) and show distinct areas of higher and lower grades (Fig. 7A). A trend of rising copper content is visible over several hundreds of metres along strike of the Kirilabombwe anticline, culminating in grades exceeding 5 wt% in the hinge zone of this anticline and in the fault zone parallel to its axial plane. Compared to these high values, average values in the mine are much lower. In the hinge zone, bornite and chalcocite are often abundantly present in the Ore Shale, forming aggregated stringers of sulphides. The petrographic study of samples from these areas show that both hypogene and supergene chalcocite occur. Most chalcocite is supergene and is often associated with goethite or hematite rims, in dolomitic bands and is frequently related to secondary porosity. The dolomitic bands are often very porous and ground conditions in this area are very poor leading to modification of the overcut and bench mining methods (Lipalile et al., 2005). Samples that were collected farther south of the hinge zone (4100–4300 mN at 1000 m depth level) do not show this same abundance of secondary chalcocite and are instead dominated by chalcopyrite and bornite as well as being less porous. This coincides with diminishing copper contents at increasing distance away from the fold hinge (Fig. 7A).

Total copper contents are also high (>5 wt%) in the proximity of the fault zones on the southern limb of the anticline (Fig. 7A). Grades are over 5 wt% at the 2200 mN fault zone and decrease over several hundred metres to the north and south of this zone. The influence of the 2700 mN fault zone on the copper content is not as strong as the larger axial plane fault zone and the 2200 mN fault zone. Macro- and microscopically the rocks in proximity to individual faults show intense weathering and abundant supergene mineralisation (e.g. for ~15 m for a fault at 2718 mN). This mineralisation is present as secondary chalcocite and malachite in stringers along bedding planes, pervasive in the matrix or as pore infill. Where dolomitic bands occur, they are often very porous and associated with chalcocite and goethite that fills up the pores. Acid soluble copper contents are high (>1 wt%) near the 2200 mN fault zone, contributing to the high total copper contents. Acid soluble copper can be associated with minerals such as malachite, azurite and chrysocolla. Other fault zones, however, do not contain notably higher acid soluble copper contents (<0.5 wt%).

A smaller zone of secondary parasitic folds on the southern limb of the Kirilabombwe anticline (180 mN–600 mS at 1 km depth) shows slightly elevated but variable copper grades between 2 and 5 wt% (Fig. 7A). The zone contains low amplitude north to northwest plunging folds. Economic mineralisation (>1 wt%) extends over 1 m into the footwall formations in these areas. Other authors noted similar ore distribution patterns in the same zone of secondary folding, at much higher excavation levels (150–350 m below surface; Fleischer et al., 1976; Ralston, 1963; Schwellnus, 1961). The same pattern of mineralisation extending into footwall formations also occurs around the fold hinge of the Kirilabombwe anticline (~1–2 m). Farther away from the fold hinge, footwall formations are less or not economically mineralised.

Average values of cobalt are higher than 0.05 wt% (Fig. 7B). The different fault zones show a marked influence on total cobalt concentrations as cobalt is severely leached in the proximity (~50 m) to all fault zones. Lower cobalt concentrations are also present between the two fault zones on the southern limb of the Kirilabombwe anticline (Fig. 7B). It therefore appears that cobalt was leached preferentially from areas with high permeability. The area between the two fault zones (2200 mN and 2700 mN) is affected by Co leaching while the area to the north of the 2200 mN fault zone does not show any effects (Fig. 7B). Carrollite has been observed in this study and trace amounts of cobaltian pyrite are present at the mine (Konkola Copper Mines, 2010). Sweeney et al. (1986) have measured up to 4.9 wt% of cobalt in dolomite. Based upon this study alone, however, it is not possible to attribute the leaching or enrichment of cobalt to certain mineral phases.

7. Sulphur isotopic composition

7.1. Methodology

Using a diamond pin, areas between 300 and 600 μm of homogeneous sulphide were highlighted under a reflected light microscope. Selected areas of samples were combusted in situ at 2000 °C with a Nd:YAG laser (Spectron Lasers 902Q CW) in an evacuated chamber containing a volume of excess oxygen used to generate $SO_{2(g)}$ following the technique of Wagner et al. (2002). The released $SO_{2(g)}$ was measured using an online VG SIRA II mass spectrometer. Analytical precision was around ±0.2‰, with calibration of the mass spectrometer by repeated measurements of an internal laboratory standard CP-1 (chalcopyrite), and two international standards NBS-123 (sphalerite) and IAEA-S-3 (Ag_2S). All values are reported in per mil deviation (‰) from the Vienna Canyon Diablo Troilite (V-CDT) standard.

7.2. Results and interpretation

Sulphur isotope compositions were determined on chalcopyrite (n = 17) and secondary chalcocite (n = 6) from the Ore Shale formation at several locations in the mine (Table 2). All $\delta^{34}S$ values lie between −8.7‰ and +2.0‰ V-CDT (Fig. 8). The $\delta^{34}S$ values for chalcopyrite range between −8.7‰ and +1.4‰ V-CDT and values for chalcocite between −4.4‰ and +2.0‰ V-CDT. Measured chalcopyrite occurred (1) disseminated in the host rock, (2) in cemented lenses and (3) in layer-parallel and irregular veins. The analysed chalcocite minerals were all secondary.

The sulphur isotope compositions for all of the analysed sulphides lie within the range reported by Sweeney et al. (1986) and are slightly lower than those reported by Dechow and Jensen

Table 2
S isotope data of different sulphide types. cc = chalcocite; cpy = chalcopyrite; D = disseminated in host rock; C = cemented lenses or layers; L = layer-parallel vein; I = irregular vein. All sulphide isotope measurements were carried out on polished sections of hand specimens of different units of the Ore Shale formation. Column 'Unit' indicates the different units of the Ore Shale formation. The samples were taken from fresh surfaces in recently developed underground mining crosscuts.

Sample	$\delta^{34}S$ ‰ V-CDT	Unit	Position	Sulphide	Type
KM10KT07	−4.4	B	4300 mN	cc	D
KM10KT07	−4.2	B	4300 mN	cc	D
KM10KT16	−3.6	D	MOCB	cc	D
KM10KT16	−2.6	D	MOCB	cc	D
KM10KT30	2.0	A	190 mS	cc	D
KM10KT30	1.3	A	190 mS	cc	D
KM10KT43	−4.1	E	4100 mN	cpy	L
KM10KT43	−3.3	E	4100 mN	cpy	L
KM10KT45	−4.7	E	4100 mN	cpy	L
KM10KT50	−4.6	D	MOCB	cpy	I
KM10KT50	−5.0	D	MOCB	cpy	I
KM10KT52	−7.6	D	171 mN	cpy	D
KM10KT52	−8.7	D	171 mN	cpy	L
KM10KT52	−8.5	D	171 mN	cpy	L
KM10JG28	1.4	E	850 mS	cpy	C
KM10JG46	−1.1	C/D	190 mS	cpy	C
KM10JG46	−1.0	C/D	190 mS	cpy	D
KM10JG55	−1.6	C	4300 mN	cpy	D
KM10JG55	−2.4	C	4300 mN	cpy	L
KM10JG56	−2.5	C	4300 mN	cpy	L
KM10JG56	−2.0	C	4300 mN	cpy	C
KM10JG58	−4.8	D	4100 mN	cpy	D
KM10JG58	−4.6	D	4100 mN	cpy	D

(1965) for sulphides at Konkola. The isotopic signatures are not affected by large scale isotope homogenisation because this occurs at higher metamorphic grades - upper amphibolites facies metamorphism – than the conditions the Konkola area has experienced (Crowe et al., 1990). Sulphide is interpreted to originate either from direct reduction of seawater sulphate $\left(SO_4^{2-}\right)$ or the dissolution of evaporate sulphates (cf. El Desouky et al., 2010). The latter is indicated by the presence of evaporitic nodules and layers in the Lower Roan Group sediments (Cailteux et al., 1994; Jackson et al., 2003), the arid sedimentary environment and the absence of evidence for a widespread magmatic source for sulphur in the Zambian Copperbelt (Selley et al., 2005). It is improbable that all of the S was derived from in situ dissolution of evaporitic nodules, given the very small amount of pseudomorphosed nodules that were observed throughout the mine, contrary to the interpretation of Sweeney et al. (1986). It is also unlikely that reduced S and reaction products of sulphate reduction were capable of being transported for long distances (Haest et al., 2009; Muchez et al., 2008). Hence, if extra S was added to the system, it was likely reduced in situ.

Fluctuations of $\delta^{34}S$ for marine sulphates between 840 Ma and the Sturtian glaciations range between +17.5‰ and +19.0‰ V-CDT (Gorjan et al., 2000; Hurtgen et al., 2002, 2005; Veizer et al., 1980). Assuming a marine or evaporitic source with a $\delta^{34}S_{sulphate}$ of +17.5‰ V-CDT, the fractionation during reduction to sulphide falls between 15.5‰ and 26.2‰ for all sulphides at Konkola. Fractionation of sulphides in the host rock and cemented lenses lies between 18.6‰ and 25.6‰ V-CDT.

8. Discussion

8.1. Evidence for remobilisation

The petrographic study shows that some of the smaller sulphides in cemented lenses are overgrown by authigenic quartz and feldspar. Metamorphic phyllosilicates crosscut these overgrowths and small sulphides (Fig. 5D). Based upon these relationships, some of the sulphides were clearly precipitated pre-metamorphism and during diagenesis, but their age cannot be further constrained based upon this study. The bulk of the sulphides, however, postdate biotite (Fig. 5C), implying that the majority of sulphides in the cemented lenses, were precipitated during or after metamorphism. At Konkola North (Fig. 2), unoriented coarse biotite postdates fine-grained biotite and rock foliation and is coeval with sulphide mineralisation (Sutton and Maynard, 2005). These authors suggest that the unoriented biotite postdates low grade metamorphism and possibly deformation and also point to a relatively late mineralisation event. At Musoshi, secondary biotite and muscovite are intergrown with sulphides and also interpreted to be coeval with sulphide precipitation (Richards et al., 1988) which is in agreement with observations at Konkola. No definitive crosscutting relationships could be determined for the disseminated sulphides in the Ore Shale formation and, in general, the timing of disseminated mineralisation in the Copperbelt is not established (Sillitoe et al., 2010).

Sulphur isotope fractionation during reduction of sulphides in the host rock and cemented lenses lies between 18.6‰ and 25.6‰ V-CDT. These fractionation values are in agreement with bacterial sulphate reduction (BSR) in a relatively closed environment (Machel, 2001; Machel et al., 1995). Although thermochemical sulphate reduction cannot be ruled out for fractionations up to 20‰ (Machel et al., 1995), it can be definitely ruled out for fractionations beyond this, and so is unlikely to be the principal mechanism for producing sulphides at Konkola. Nonetheless, it is impossible for the veins, which clearly formed under greenschist metamorphic conditions, to contain primary bacteriogenic sulphide. Taking into account the similar $\delta^{34}S$ between the different vein generations and earlier sulphides, we propose that remobilisation of sulphur from early diagenetic sulphides has led to these similarities – the most parsimonious explanation. This interpretation is in agreement with observations from the petrography, showing similar mineralogy in multiple sulphide generations (Fig. 4). The remobilisation of earlier sulphides has been recognised in several other deposits of the Copperbelt (Annels, 1989; Cailteux et al., 2005; Lerouge et al., 2005). In addition, the $\delta^{34}S$ values show little variation within the same sample between vein sulphides and disseminated sulphides in host rock (e.g. for sample KM10KT52 in Table 2), which was also observed by Sweeney et al. (1986) for lenticle sulphides and disseminated sulphides. Considering the relationship between $\delta^{34}S$ and the different units in the Ore Shale formation, units D and E show generally lower $\delta^{34}S$ values as opposed to relatively higher values in unit C (Fig. 8). This is exactly opposite to the trends observed by other authors for Konkola and casts some doubt on the interpretation of changing $\delta^{34}S$ fractionation with transgressive/regressive cycles at Konkola by Sweeney et al. (1986).

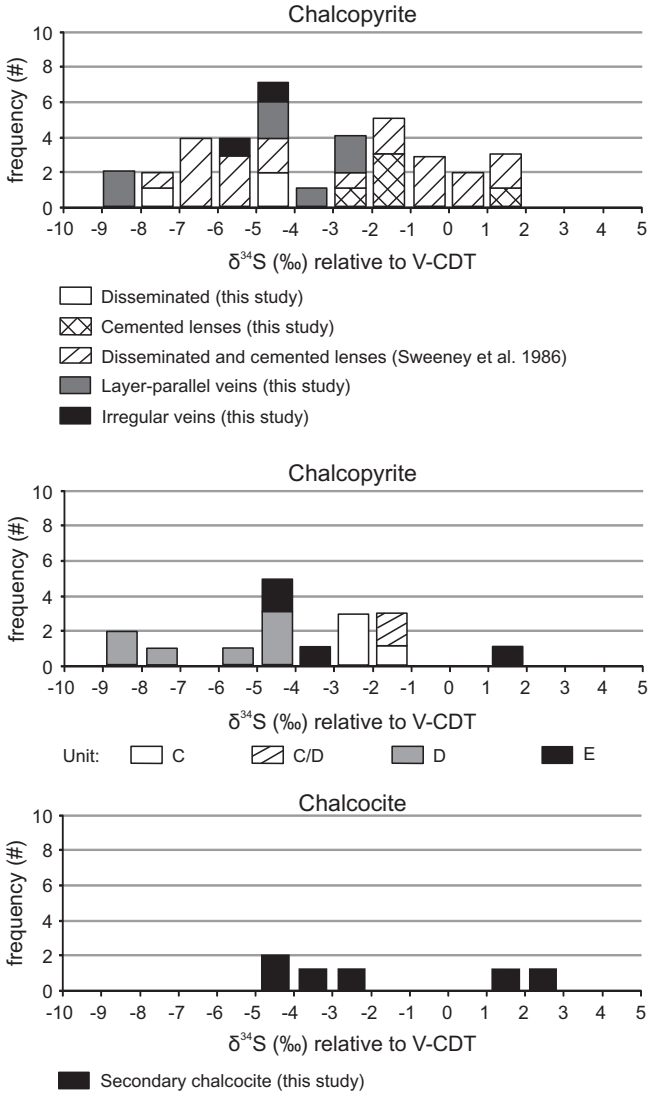

Fig. 8. $\delta^{34}S$ values (‰) relative to V-CDT for measurements of chalcopyrite from different mineralising phases (top), of different units of the Ore Shale formation (middle) and of secondary chalcocite (bottom). Values from Sweeney et al. (1986) are shown for comparison (top).

8.2. Formation of veins

It is difficult to place exact time constraints on the formation of the layer-parallel and irregular veins but the occurrence of biotite in these veins implies emplacement during metamorphism. The opening of cracks in the host rock perpendicular to bedding require the least effective stress in a system (σ'_3) to be vertical as extensional forces need to be applied perpendicular to bedding. This is indicated by the occurrence of elongated dolomite crystals in some layer-parallel veins that are interpreted to be aligned with σ'_3 (Fig. 5F). Layer-parallel veins at Konkola are often formed at the contacts between coarse-grained and fine-grained zones. Pre-folding layer-parallel veins preferentially developing on sites of contrasting competence have been observed in other orogenic belts such as the High-Ardenne slate belt (Van Noten et al., 2011) and the Rhenish Massif in Germany (de Roo and Weber, 1992) or in other settings (Fitches et al., 1986; Hilgers et al., 2006; Jessell et al., 1994). Layer-parallel veins are often found in basins with alternating beds and can form by the building up of fluid pressure until overpressures are reached (Cosgrove, 2001; Sibson, 2003; Van Noten et al., 2011). These veins can form before folding, during burial (Fitches et al., 1986), at the onset of folding (Cosgrove, 2001; Hilgers et al., 2006) or even during folding (Tanner, 1989). Therefore, the layer-parallel veins were most likely formed just before or during compressive folding during the Lufilian orogeny. Similar layer-parallel veins with a quartz-dolomite-sulphide mineralogy are also recognised at Nchanga (McGowan et al., 2006) and Nkana (Brems et al., 2009; Muchez et al., 2010) and are often found in several other fine-grained Zambian deposits (Selley et al., 2005). Based upon the crosscutting relationships, the irregular veins at Konkola most likely formed during or after the main phases of compressional deformation at high fluid pressures (cf. Sibson, 2004).

8.3. Metamorphism and deformation

Detrital muscovite in the Ore Shale formation is generally aligned bedding parallel. This foliation is interpreted to be related to compaction and burial, as it was estimated that ~6000 m of Katanga Supergroup sedimentary rocks were deposited at maximum burial in the basin (Cailteux et al., 2005). The presence of abundant biotite and the assemblage of quartz, dolomite, biotite, muscovite and chlorite indicate biotite zone greenschist facies metamorphism (Best, 2003). These observations are in agreement with the literature which suggests prograde greenschist facies metamorphism for the Konkola region (Cosi et al., 1992; Kampunzu et al., 2000; Key et al., 2001; Ridgway and Ramsay, 1986). Fan-shaped chlorite replacing biotite is interpreted to represent retrograde metamorphism passing through greenschist facies metamorphic conditions, as has been proposed for other parts of the Zambian Copperbelt (Unrug, 1988).

Variable but frequent tabular twinning of dolomite occurs at the Konkola deposit, with individual twin width in dolomite up to 10 μm in size. Dolomite twinning does not develop at conditions <300 °C, rendering a lower temperature limit during deformation (Barber and Wenk, 2001; Passchier and Trouw, 2005). Quartz shows variable undulose extinction and occasionally the development of subgrain boundaries, in agreement with relatively low deformation at Konkola (cf. Faleiros et al., 2010; Stipp et al., 2002). Several types of exsolution lamellae are found in ore minerals at Konkola. Metamorphism can have a significant effect on ore textures and ore grain size and the behaviour of different sulphide minerals during metamorphism can vary to a great extent (Craig and Vokes, 1993; Larocque and Hodgson, 1995; Marshall and Gilligan, 1987). This could explain the variety of alteration and replacement textures observed in hypogene mineralisation at Konkola.

8.4. Supergene processes

In addition to hypogene mineralisation, supergene processes are important at the Konkola deposit. Many of the replacement textures on the edges of the ore minerals are typical for oxidation of sulphides (Craig and Vaughan, 1994; Ramdohr, 1980; Sillitoe, 2005). Often iron depleted rims of chalcocite, digenite and covellite are found on the edges of chalcopyrite and bornite (Fig. 6B). The iron is removed in solution and reprecipitates in oxidised forms such as goethite along cracks or in voids (Fig. 6A; Craig and Vaughan, 1994). At Konkola, secondary chalcocite is abundant in areas with high permeability such as fault zones. Chalcocite commonly occurs in both hypogene and supergene environments (Sillitoe, 2005; Vaughan and Craig, 1997) and the timing of chalcocite in the paragenesis of ore deposits is often uncertain (Selley et al., 2005; Sillitoe, 2005). Sulphur isotope values for supergene chalcocite (−4.4‰ to +2.0‰ V-CDT) are comparable to or slightly higher than hypogene sulphides (Fig. 8). They show fractionation between 15.5‰ and 21.9‰ V-CDT and are also most readily explained by local remobilisation of earlier sulphide phases. Data from several ore deposits and theoretical modelling point to direct inheritance of S and its isotopic signature during supergene weathering, without the need for major external S sources (Ague and Brimhall, 1989; Cook and Spry, 1999; Field and Gustafson, 1976; Sillitoe, 2005).

Another important supergene mineral at Konkola is malachite. The textures and habits of malachite at the deposit are very similar to other occurrences in the Copperbelt (De Putter et al., 2010). When structural permeability is high, oxidation of hypogene sulphides can occur very deep (Ague and Brimhall, 1989; Sillitoe, 2005). Supergene enrichment and leaching by supergene fluid circulation occurs at depths of up to 1 km from the present-day surface at Konkola. Partial sulphide oxidation up to depths of ~750 m is common in the Zambian Copperbelt (Fleischer et al., 1976).

8.5. Structural control

The close relationship between macro- and meso-scale structural features with higher copper and lower cobalt grades implies a strong structural control on the ore grade and suggests that these structures played a significant role in the (re)mobilisation and subsequent concentration of the metals.

These observations have also been made for several other deposits of the Central African Copperbelt. At Nkana South, stratiform orebodies (cutoff at 1 wt% copper) are situated in the hinge zones of fold structures (Brems et al., 2009). These intensely deformed, very tight to isoclinal folds have the same structural trend (NW–SE) as those in Konkola, gently plunging to the NW. At the Nchanga deposit, McGowan et al. (2006) reported a strong correlation between ore mineralisation and NE verging fault propagation folds, thrusts and basal detachments. These folds also have WNW–ESE striking fold axes that plunge gently to the WNW. The geometry of the folds at Konkola is in agreement with the regional tectonic and structural style. The Domes region consists mainly of upright to slightly inclined NW–SE trending folds that dominate the structural style (Cosi et al., 1992; Selley et al., 2005). Tectonic transport was interpreted to be towards the northeast (Kampunzu and Cailteux, 1999; Porada and Berhorst, 2000), which is in agreement with the folding geometry recognised at Konkola. Deposits in the western part of the Lufilian belt are often located at the intersection of Roan Group sediments and structural lineaments (Dewaele et al., 2006). These lineaments are interpreted to play an important role in the migration of supergene fluids. The importance of steep through going faults for supergene oxidation, leaching and enrichment is also highlighted at Konkola, as these provide the necessary permeability for internal mobilisation of the base metals (cf. Marshall and Gilligan, 1987; Sillitoe, 2005).

From the grade maps it appears that especially cobalt was leached preferentially from areas with high permeability. The area between the two fault zones at 2200 mN and 2700 mN is affected by Co leaching while the area to the north of the 2200 mN fault zone does not show any effect (Fig. 7B). Not all faults are permeable and some can indeed act as impermeable barriers that lead to deeper supergene enrichment and leaching on one side of the fault (Sillitoe, 2005). It is apparent that Cu and Co do not behave in the same way relative to structural features in the area (Fig. 7). This is likely the result of different geochemical behaviour of these two elements during supergene conditions (Chivot et al., 2008; Decrée et al., 2010; Katsikopoulos et al., 2008; Rose, 1989). Decoupling of Cu and Co is recognised in other deposits of the Central African Copperbelt. In the Tenke-Fungurume Cu–Co district, the ore distribution in shallow Roan Group rocks resulted from supergene oxidation and Cu–Co decoupling during transport, superimposed on hypogene sulphide ore (Fay and Barton, 2012). These authors interpreted this to be due to solubility differences of Cu and Co under supergene conditions in zones of enhanced permeability. A further example is the frequent occurrence of cobalt caps in the D.R.Congo where separation of Co rich caps and deeper Cu enrichment are shown to result from different precipitation and dissolution mechanisms for malachite and heterogenite (De Putter et al., 2010; Decrée et al., 2010).

9. Conclusions

Using a mine-scale approach and studying several boreholes and underground crosscuts, this study indicates that the Cu–Co ore at the Konkola deposit is not only diagenetic in origin but that significant ore precipitation, recrystallisation and remobilisation occurred before, during and after the main stages of the Lufilian orogeny. Copper and cobalt grade maps indicate that there is significant structural control on the ore grade distribution. Macro- and mesoscale structural features played an important role in the concentration of the metals and upgrading of the ore deposit, certainly during supergene processes. A detailed petrographic study revealed that the hypogene Cu–Co mineralisation at Konkola occurs disseminated in the host rock, in cemented lenses and in layer-parallel and irregular veins. Some sulphides in cemented lenses predate biotite zone greenschist facies metamorphism as constrained by the growth of metamorphic biotite. However, most sulphides in cemented lenses were precipitated during or after metamorphism. Layer-parallel veins formed after burial diagenesis, just before or during compressive folding. Irregular veins crosscutting the layer-parallel veins formed at high fluid pressures during or after compressional deformation. Deep supergene enrichment and leaching occurs up to a km in depth, mainly in the form of secondary chalcocite, goethite and malachite and is often associated with zones of high permeability. Similarities in sulphur isotope signatures between different phases of hypogene and supergene sulphides in the Ore Shale formation indicate remobilisation of earlier sulphides to form later sulphides, strongly supported by petrographic evidence.

Acknowledgements

We are grateful to the geologists at Konkola Copper Mines Plc., especially Davy Mubita, Sebastian Haabanyama, Sachin Velhal, Godfrey Chagondah, Gautam Murlidhar, Daniel Maunge and Phiri Cryton for the practical arrangements, access to the mine and data and stimulating discussions. We thank Herman Nijs for the careful preparation of thin and polished sections. We gratefully acknowledge the constructive comments of two anonymous reviewers. This research is financially supported by research Grant G.0414.08 of the FWO-Vlaanderen. Koen Torremans and Johanna Gauquie benefited from a travel grant of the Vlaamse Interuniversitaire Raad (VLIR-UOS).

References

Ague, J.J., Brimhall, G.H., 1989. Geochemical modeling of steady state fluid flow and chemical reaction during supergene enrichment of porphyry copper deposits. Economic Geology 84, 506–528.

Annels, A.E., 1989. Ore genesis in the Zambian Copperbelt, with particular reference to the Northern Sector of the Chambishi Basin. In: Boyle, R.W., et al. (Eds.), Sediment-Hosted Stratiform Copper Deposits. Geological Society of Canada, pp. 427–452.

Armstrong, R.A., Master, S., Robb, L.J., 2005. Geochronology of the Nchanga Granite, and constraints on the maximum age of the Katanga Supergroup, Zambian Copperbelt. Journal of African Earth Sciences 42, 32–40.

Barber, D.J., Wenk, H.-R., 2001. Slip and dislocation behaviour in dolomite. European Journal of Mineralogy 13, 221–243.

Batumike, M.J., Kampunzu, A.B., Cailteux, J.L.H., 2006. Petrology and geochemistry of the Neoproterozoic Nguba and Kundelungu Groups, Katangan Supergroup, southeast Congo: implications for provenance, paleoweathering and geotectonic setting. Journal of African Earth Sciences 44, 97–115.

Batumike, M.J., Cailteux, J.L.H., Kampunzu, A.B., 2007. Lithostratigraphy, basin development, base metal deposits, and regional correlations of the Neoproterozoic Nguba and Kundelungu rock successions, central African Copperbelt. Gondwana Research 11, 432–447.

Best, M.G., 2003. Igneous and Metamorphic Petrology, second ed. Blackwell Science.

Brems, D., Muchez, P., Sikazwe, O., Mukumba, W., 2009. Metallogenesis of the Nkana copper–cobalt South orebody, Zambia. Journal of African Earth Sciences 55, 185.

Bull, S., Selley, D., Broughton, D., Hitzman, M., Cailteux, J., Large, R., McGoldrick, P., 2011. Sequence and carbon isotopic stratigraphy of the Neoproterozoic Roan Group strata of the Zambian copperbelt. Precambrian Research 190, 70–89.

Cailteux, J., Binda, P.L., Katekesha, W.M., Kampunzu, A.B., Intiomale, M.M., Kapenda, D., Kaunda, C., Ngongo, K., Tshiauka, T., Wendorff, M., 1994. Lithostratigraphical correlation of the Neoproterozoic Roan Supergroup from Shaba (Zaire) and Zambia, in the central African copper–cobalt metallogenic province. Journal of African Earth Sciences 19, 265–278.

Cailteux, J.L.H., Kampunzu, A.B., Lerouge, C., Kaputo, A.K., Milesi, J.-P., 2005. Genesis of sediment-hosted stratiform copper–cobalt deposits, central African Copperbelt. Journal of African Earth Sciences 42, 134–158.

Cailteux, J.L.H., Kampunzu, A.B., Lerouge, C., 2007. The Neoproterozoic Mwashya–Kansuki sedimentary rock succession in the central African Copperbelt, its Cu–Co mineralisation, and regional correlations. Gondwana Research 11, 414–431.

Chivot, J., Mendoza, L., Mansour, C., Pauporté, T., Cassir, M., 2008. New insight in the behaviour of Co–H_2O system at 25–150 °C, based on revised Pourbaix diagrams. Corrosion Science 50, 62–69.

Clark, D.J., Gemmell, J.B., Norman, M., Hespe, A.M., 2001. Textural and geochemical distinction between supergene and hypogene Cu sulfide phases at the Mammoth copper deposit, Queensland, Australia. In: Piestrzynski, et al. (Eds.), Mineral Deposits at the Beginning of the 21st Century, Swets & Zeitlinger Publishers, Lisse, pp. 219–222.

Cook, N.J., Spry, P.G., 1999. Sulphur isotope characteristics of remobilised ores from the Bleikvassli Zn–Pb–(Cu) deposit, Nordland, Norway. In: Stanley, C.J., et al. (Eds.), Mineral Deposits: Processes to Processing: Proceedings of the Fifth Biennial SGA Meeting and the 10th Quadrenial IAGOD Symposium, vol. 1, London, United Kingdom, A.A. Balkema, Rotterdam, pp. 939–942.

Cosgrove, J.W., 2001. Hydraulic fracturing during the formation and deformation of a basin: a factor in the dewatering of low-permeability sediments. AAPG Bulletin 85, 737–748.

Cosi, M., De Bonis, A., Gosso, G., Hunziker, J., Martinotti, G., Moratto, S., Robert, J.P., Ruhlman, F., 1992. Late Proterozoic thrust tectonics, high-pressure metamorphism and uranium mineralization in the Domes Area, Lufilian Arc, Northwestern Zambia. Precambrian Research 58, 215–240.

Craig, J.R., Vaughan, D.J., 1994. Ore Microscopy & Ore Petrography. John Wiley & Sons, Inc..

Craig, J.R., Vokes, F.M., 1993. The metamorphism of pyrite and pyritic ores: an overview. Mineralogical Magazine 57, 3–18.

Crowe, D.E., Valley, J.W., Baker, K.L., 1990. Micro-analysis of sulfur-isotope ratios and zonation by laser microprobe. Geochimica et Cosmochimica Acta 54, 2075–2092.

De Putter, T., Mees, F., Decrée, S., Dewaele, S., 2010. Malachite, an indicator of major Pliocene Cu remobilization in a karstic environment (Katanga, Democratic Republic of Congo). Ore Geology Reviews 38, 90–100.

de Roo, J.A., Weber, K., 1992. Laminated veins and hydrothermal breccia as markers of low-angle faulting, Rhenish Massif, Germany. Tectonophysics 208, 413–430.

De Waele, B., Johnson, S.P., Pisarevsky, S.A., 2008. Palaeoproterozoic to Neoproterozoic growth and evolution of the eastern Congo Craton: its role in the Rodinia puzzle. Precambrian Research 160, 127–141.

Dechow, E., Jensen, M.L., 1965. Sulfur isotopes of some central African sulfide deposits. Economic Geology 60, 894–941.

Decrée, S., Deloule, É., Ruffet, G., Dewaele, S., Mees, F., Marignac, C., Yans, J., De Putter, T., 2010. Geodynamic and climate controls in the formation of Mio–

Pliocene world-class oxidized cobalt and manganese ores in the Katanga province, DR Congo. Mineralium Deposita 45, 621–629.
Dewaele, S., Muchez, P., Vets, J., Fernandez-Alonzo, M., Tack, L., 2006. Multiphase origin of the Cu–Co ore deposits in the western part of the Lufilian fold-and-thrust belt, Katanga (Democratic Republic of Congo). Journal of African Earth Sciences 46, 455–469.
El Desouky, H.A., Muchez, P., Boyce, A., Schneider, J., Cailteux, J., Dewaele, S., Von Quadt, A., 2010. Genesis of sediment-hosted stratiform copper–cobalt mineralization at Luiswishi and Kamoto, Katanga Copperbelt (Democratic Republic of Congo). Mineralium Deposita 45, 735–763.
Faleiros, F.M., Campanha, G.A.C., Bello, R.M.S., Fuzikawa, K., 2010. Quartz recrystallization regimes, *c*-axis texture transitions and fluid inclusion reequilibration in a prograde greenschist to amphibolite facies mylonite zone (Ribeira Shear Zone, SE Brazil). Tectonophysics 485, 193–214.
Fay, I., Barton, M., 2012. Alteration and ore distribution in the Proterozoic Mines Series, Tenke-Fungurume Cu–Co district, Democratic Republic of Congo. Mineralium Deposita 47, 501–519.
Field, C.W., Gustafson, L.B., 1976. Sulfur isotopes in the porphyry copper deposit at El Salvador, Chile. Economic Geology 71, 1533–1548.
Fitches, W.R., Cave, R., Craig, J., Maltman, A.J., 1986. Early veins as evidence of detachment in the Lower Palaeozoic rocks of the Welsh Basin. Journal of Structural Geology 8, 607–620.
Fleet, M.E., 2006. Phase equilibria at high temperatures. In: Vaughan, D.J. (Ed.), Sulfide Mineralogy & Geochemistry. Mineralogical Society of America, pp. 365–420.
Fleischer, V.D., Garlick, W.G., Haldane, R., 1976. Geology of the Zambian copper belt. In: Wolf, K.H. (Ed.), Handbook of Strata-bound and Stratiform Ore Deposits, 6. Elsevier, New York, pp. 223–352.
Gorjan, P., Veevers, J.J., Walter, M.R., 2000. Neoproterozoic sulfur-isotope variation in Australia and global implications. Precambrian Research 100, 151–179.
Haest, M., Muchez, P., 2011. Stratiform and vein-type deposits in the Pan-African Orogen in Central and Southern Africa: evidence for multiphase mineralisation. Geologica Belgica 14, 23–44.
Haest, M., Muchez, P., Dewaele, S., Boyce, A., von Quadt, A., Schneider, J., 2009. Petrographic, fluid inclusion and isotopic study of the Dikulushi Cu–Ag deposit, Katanga (D.R.C.): implications for exploration. Mineralium Deposita 44, 505–522.
Hilgers, C., Kirschner, D.L., Breton, J.P., Urai, J.L., 2006. Fracture sealing and fluid overpressures in limestones of the Jabal Akhdar dome, Oman mountains. Geofluids 6, 168–184.
Hitzman, M., Kirkham, R., Broughton, D., Thorson, J., Selley, D., 2005. The sediment-hosted stratiform copper ore system. Economic Geology 100th Anniversary Volume, 609–642.
Hurtgen, M.T., Arthur, M.A., Suits, N.S., Kaufman, A.J., 2002. The sulfur isotopic composition of Neoproterozoic seawater sulfate: implications for a snowball Earth? Earth and Planetary Science Letters 203, 413–429.
Hurtgen, M.T., Arthur, M.A., Halverson, G.P., 2005. Neoproterozoic sulfur isotopes, the evolution of microbial sulfur species, and the burial efficiency of sulfide as sedimentary pyrite. Geology 33, 41–44.
Jackson, M.P.A., Warin, O.N., Woad, G.M., Hudec, M.R., 2003. Neoproterozoic allochthonous salt tectonics during the Lufilian orogeny in the Katangan Copperbelt, central Africa. Geological Society of America Bulletin 115, 314–330.
Jessell, M.W., Willman, C.E., Gray, D.R., 1994. Bedding parallel veins and their relationship to folding. Journal of Structural Geology 16, 753–767.
John, T., Schenk, V., Mezger, K., Tembo, F., 2004. Timing and PT evolution of whiteschist metamorphism in the Lufilian Arc–Zambezi Belt orogen (Zambia): implications for the assembly of Gondwana. The Journal of Geology 112, 71–90.
Kampunzu, A.B., Cailteux, J.L.H., 1999. Tectonic evolution of the Lufilian Arc (Central Africa Copper Belt) during Neoproterozoic Pan African orogenesis. Gondwana Research 2, 401–421.
Kampunzu, A.B., Tembo, F., Matheis, G., Kapenda, D., Huntsman-Mapila, P., 2000. Geochemistry and tectonic setting of mafic igneous units in the Neoproterozoic Katangan Basin, Central Africa: implications for Rodinia break-up. Gondwana Research 3, 125–153.
Katongo, C., 2005. Ground conditions and support systems at 1 Shaft, Konkola mine, Chililabombwe, Zambia. In: Proceedings of the Third Southern African Conference on Base Metals. The South African Institute of Mining and Metallurgy, Kitwe, Zambia, pp. 253–280.
Katsikopoulos, D., Fernández-González, Á., Prieto, A.C., Prieto, M., 2008. Co-crystallization of Co(II) with calcite: implications for the mobility of cobalt in aqueous environments. Chemical Geology 254, 87–100.
Key, R.M., Liyungu, A.K., Njamu, F.M., Somwe, V., Banda, J., Mosley, P.N., Armstrong, R.A., 2001. The western arm of the Lufilian Arc in NW Zambia and its potential for copper mineralisation. Journal of African Earth Sciences 33, 503–528.
Konkola Copper Mines, 2010. Unpublished Reports. Geological Maps, Borehole Reports, 1:250 Mine Maps and Cu–Co Assay Results, Chililabombwe, Zambia.
Larocque, A.C.L., Hodgson, C.J., 1995. Effects of greenschist-facies metamorphism and related deformation on the Mobrun massive sulfide deposit, Québec, Canada. Mineralium Deposita 30, 439–448.
Lerouge, C., Cailteux, J.H., Kampunzu, A.B., Milesi, J.P., Fléhoc, C., 2005. Sulphur isotope constraints on formation conditions of the Luiswishi ore deposit, Democratic Republic of Congo (DRC). Journal of African Earth Sciences 42, 173–182.
Lipalile, M., Naismith, A.W., Tunono, A.B., 2005. Geotechnical considerations in the design of the MOCB mining method at Konkola No. 3 shaft. Journal of the South African Institute of Mining and Metallurgy 105, 607–614.
Machel, H.G., 2001. Bacterial and thermochemical sulfate reduction in diagenetic settings—old and new insights. Sedimentary Geology 140, 143–175.
Machel, H.G., Krouse, H.R., Sassen, R., 1995. Products and distinguishing criteria of bacterial and thermochemical sulfate reduction. Applied Geochemistry 10, 373–389.
Marshall, B., Gilligan, L.B., 1987. An introduction to remobilization: information from ore-body geometry and experimental considerations. Ore Geology Reviews 2, 87–131.
Master, S., Wendorff, M., 2011. Neoproterozoic glaciogenic diamictites of the Katanga Supergroup, Central Africa. Geological Society, London, Memoirs 36, 173–184.
Master, S., Rainaud, C., Armstrong, R.A., Phillips, D., Robb, L.J., 2005. Provenance ages of the Neoproterozoic Katanga Supergroup (Central African Copperbelt), with implications for basin evolution. Journal of African Earth Sciences 42, 41–60.
McGowan, R., Roberts, S., Boyce, A., 2006. Origin of the Nchanga copper–cobalt deposits of the Zambian Copperbelt. Mineralium Deposita 40, 617–638.
Meert, J.G., Torsvik, T.H., 2003. The making and unmaking of a supercontinent: Rodinia revisited. Tectonophysics 375, 261–288.
Muchez, P., Vanderhaeghen, P., El Desouky, H., Schneider, J., Boyce, A., Dewaele, S., Cailteux, J., 2008. Anhydrite pseudomorphs and the origin of stratiform Cu–Co ores in the Katangan Copperbelt (Democratic Republic of Congo). Mineralium Deposita 43, 575–589.
Muchez, P., Brems, D., Clara, E., De Cleyn, A., Lammens, L., Boyce, A., De Muynck, D., Mukumba, W., Sikazwe, O., 2010. Evolution of Cu–Co mineralizing fluids at Nkana Mine, Central African Copperbelt, Zambia. Journal of African Earth Sciences 58, 457–474.
Mulenga, S., Fernandez-Rubio, R., Leon, A., Baquero, J., 1992. Estimation of quantitative water inflow from different sources in Konkola Mine, Zambia. Mine Water and the Environment 11, 1–22.
Passchier, C.W., Trouw, R.A.J., 2005. Microtectonics. Springer-Verlag, Berlin.
Porada, H., Berhorst, V., 2000. Towards a new understanding of the Neoproterozoic-Early Palaeozoic Lufilian and northern Zambezi Belts in Zambia and the Democratic Republic of Congo. Journal of African Earth Sciences 30, 727–771.
Rainaud, C., Master, S., Armstrong, R.A., Phillips, D., Robb, L.J., 2005. Monazite U–Pb dating and $^{40}Ar–^{39}Ar$ thermochronology of metamorphic events in the Central African Copperbelt during the Pan-African Lufilian Orogeny. Journal of African Earth Sciences 42, 183–199.
Ralston, I.T., 1963. Some structural features associated with the Bancroft orebodies. In: Lombard, J., Nicolini, P. (Eds.), Stratiform Copper Deposits in Africa, Paris. Chapter IX, 2nd Part: Tectonics. Association of African Geological Surveys, pp. 125–142.
Ramdohr, P., 1980. The Ore Minerals and Their Intergrowths. Pergamon press.
Raybould, J.G., 1978. Duplications and Related Structures of the Kirila Bombwe South Orebody. Unpublished Company Report. Nchanga Consolidated Copper Mines Ltd., Konkola Division.
Richards, J.P., Krogh, T.E., Spooner, E.T.C., 1988. Fluid inclusion characteristics and U–Pb rutile age of late hydrothermal alteration and veining at the Musoshi stratiform copper deposit, Central African copper belt, Zaire. Economic Geology 83, 118–139.
Ridgway, J., Ramsay, C.R., 1986. A provisional metamorphic map of Zambia—explanatory notes. Journal of African Earth Sciences 5, 441–446.
Rose, A.W., 1989. Mobility of copper and other heavy metals in sedimentary environments. In: Boyle, R.W., et al. (Eds.), Sediment-hosted Stratiform Copper Deposits, Geological Society of Canada Special Paper 36, pp. 97–110.
Schwellnus, J.E.G., 1961. Bancroft-Nchanga area. In: Mendelsohn, F. (Ed.), The Geology of the Northern Rhodesian Copperbelt. Macdonald and Co., London, pp. 214–233.
Selley, D., Broughton, D., Scott, R.J., Hitzman, M., Bull, S., Large, R., McGoldrick, P., Croaker, M., Pollington, N., 2005. A new look at the geology of the Zambian Copperbelt. Economic Geology 100th Anniversary Volume, 965–1000.
Sibson, R.H., 2003. Brittle-failure controls on maximum sustainable overpressure in different tectonic regimes. AAPG Bulletin 87, 901–908.
Sibson, R.H., 2004. Controls on maximum fluid overpressure defining conditions for mesozonal mineralisation. Journal of Structural Geology 26, 1127–1136.
Sillitoe, R.H., 2005. Supergene oxidized and enriched porphyry copper and related deposits. Economic Geology 100th Anniversary Volume, 723–768.
Sillitoe, R.H., Perelló, J., García, A., 2010. Sulfide-bearing veinlets throughout the stratiform mineralization of the Central African Copperbelt: temporal and genetic implications. Economic Geology 105, 1361–1368.
Stipp, M., Stünitz, H., Heilbronner, R., Schmid, S.M., 2002. The eastern Tonale fault zone: a 'natural laboratory' for crystal plastic deformation of quartz over a temperature range from 250 to 700 °C. Journal of Structural Geology 24, 1861–1884.
Sutton, S.J., Maynard, J.B., 2005. A fluid mixing model for copper mineralization at Konkola North, Zambian Copperbelt. Journal of African Earth Sciences 42, 95–118.
Sweeney, M., Binda, P.L., 1989. The role of diagenesis in the formation of the Konkola Cu–Co orebody of the Zambian Copperbelt. Geological Association of Canada Special Paper 36, 499–518.
Sweeney, M., Turner, P., Vaughan, D.J., 1986. Stable isotope and geochemical studies in the role of early diagenesis in ore formation, Konkola Basin, Zambian copper belt. Economic Geology 81, 1838–1852.
Tanner, G.P.W., 1989. The flexural-slip mechanism. Journal of Structural Geology 11, 635–655.

Tembo, F., Kampunzu, A.B., Porada, H., 1999. Tholeiitic magmatism associated with continental rifting in the Lufilian Fold Belt of Zambia. Journal of African Earth Sciences 28, 403–425.

Unrug, R., 1988. Mineralization controls and source of metals in the Lufilian fold belt, Shaba (Zaire), Zambia, and Angola. Economic Geology 83, 1247–1258.

Van Noten, K., Muchez, P., Sintubin, M., 2011. Stress-state evolution of the brittle upper crust during compressional tectonic inversion as defined by successive quartz vein types (High-Ardenne slate belt, Germany). Journal of the Geological Society 168, 407–422.

Vaughan, D.J., Craig, J.R., 1997. Sulfide ore mineral stabilities, morphologies and intergrowth textures. In: Barnes, H.L. (Ed.), Geochemistry of Hydrothermal ore Deposits. John Wiley & Sons Inc., New York, pp. 367–434.

Vedanta, 2010. Konkola Copper Mines Plc. Investor Update – January 2010. Unpublished Report. Vedanta Resources Plc.

Veizer, J., Holser, W.T., Wilgus, C.K., 1980. Correlation of $^{13}C/^{12}C$ and $^{34}S/^{32}S$ secular variations. Geochimica et Cosmochimica Acta 44, 579–587.

Wagner, T., Boyce, A.J., Fallick, A.E., 2002. Laser combustion analysis of $\delta^{34}S$ of sulfosalt minerals: determination of the fractionation systematics and some crystal-chemical considerations. Geochimica et Cosmochimica Acta 66, 2855–2863.

Wendorff, M., 2005. Sedimentary genesis and lithostratigraphy of Neoproterozoic megabreccia from Mufulira, Copperbelt of Zambia. Journal of African Earth Sciences 42, 61–81.

Wendorff, M., Key, R.M., 2009. The relevance of the sedimentary history of the Grand Conglomerat Formation (Central Africa) to the interpretation of the climate during a major Cryogenian glacial event. Precambrian Research 172, 127–142.